Support Information

A multifunctional phosphorescent iridium(III) complex for specific nucleus staining and hypoxia monitoring

Shujuan Liu,[a] Hua Liang,[a] Kenneth Yin Zhang,[a] Qiang Zhao,*[a] Xiaobo Zhou,[a] Wenjuan Xu[a] and Wei Huang*[ab]

[a] Key Laboratory for Organic Electronics and Information Displays & Institute of Advanced Materials (IAM), Jiangsu National Synergetic Innovation Center for Advanced Materials (SICAM), Nanjing University of Posts & Telecommunications, 9 Wenyuan Road, Nanjing 210023, China. E-mail: iamqzhao@njupt.edu.cn (Q. Zhao); wei-huang@njtech.edu.cn (W. Huang); Fax: (+86) 25-85866396.

[b] Key Laboratory of Flexible Electronics (KLOFE) & Institute of Advanced Materials (IAM), Jiangsu National Synergetic Innovation Center for Advanced Materials (SICAM), Nanjing Tech University (NanjingTech), 30 South Puzhu Road, Nanjing 211816, China.

Materials

All reagents and chemicals were procured from commercial sources and used without further purification. Phenanthroline (phen), 2-phenylpyridine (ppy), $IrCl_3 \bullet 3H_2O$ and phosphate buffered saline (PBS) were obtained from Acros. Cell culture reagents, fetal bovine serum (FBS) was purchased from Gibcco. Hoechst 33342 was bought from Beyotime. Metabolic inhibitors (oligomycin, 2-deoxy-D-glucose) were obtained from MCE.

General experiments

^1H NMR spectra were recorded with a Varian spectrometer at 400 MHz. Mass spectra were obtained on SHIMADZU matrix-assisted laser desorption/ionization time of flight mass spectrometer (MALDI-TOF-MASS). The UV-vis absorption spectra were recorded on a Shimadzu UV-2550 spectrometer. Steady-state emission experiments at room temperature were measured on an Edinburgh LFS-920 spectrometer. Lifetime studies were performed with an Edinburgh LFS-920 spectrometer with a hydrogen-filled excitation source. The data were analyzed by iterative convolution of the luminescence decay profile with the instrument response function using a software package provided by Edinburgh Instruments. The absolute quantum yields of the complexes were determined through an absolute method by employing an integrating sphere.

Synthesis

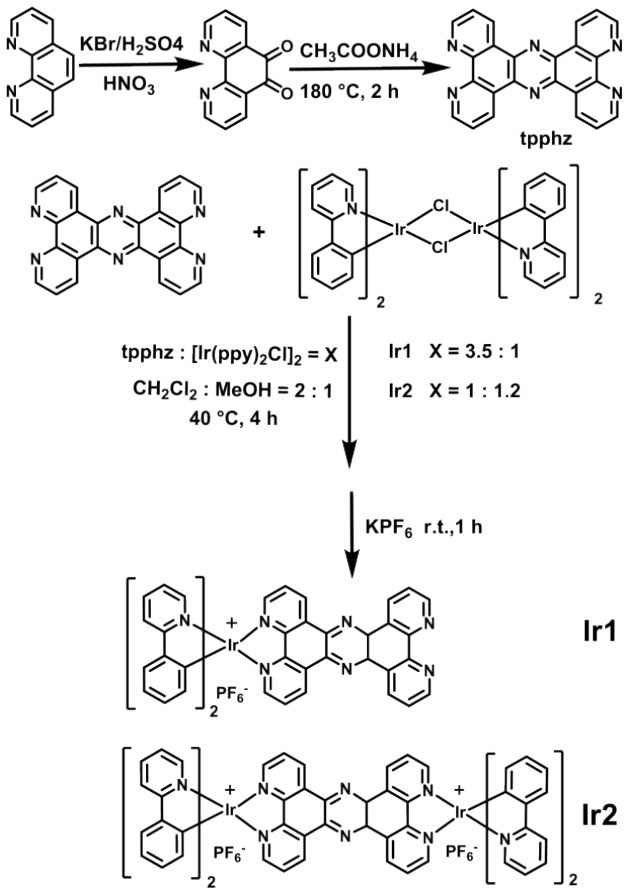

Scheme S1. The synthetic routes and structures of **Ir1** and **Ir2**.

The N^N ligand tpphz and the chloro-bridged dinuclear cyclometalated iridium(III) precursor $[Ir(ppy)_2Cl]_2$ were synthesized according to the method reported by Bolger *et al.* and Nonoyama, respectively. Both iridium(III) complexes were synthesized according to the same procedure. Herein, only the synthesis of $[Ir(ppy)_2(tpphz)]PF_6$ **(Ir1)** was described in detail. The chemical structures of **Ir1** and **Ir2** were characterized by MALDI-TOF MS and ^1H NMR. The mass spectra featured a major peak corresponding to **Ir1** and **Ir2** with one PF_6^- removed.

[Ir(ppy)$_2$(tpphz)]PF$_6$ (Ir1). A solution of $[Ir(ppy)_2Cl]_2$ (0.490 g, 0.455 mmol) and tpphz (0.050 g, 0.130 mmol) in CH_2Cl_2-MeOH (30 mL, 2:1 v/v) was heated to reflux. After 4 h, the solution was cooled down to room temperature, and then a 10-fold excess of potassium hexafluorophosphate (0.240 g, 1.3 mmol) was added. The suspension was stirred for another 1 h, and then filtered to remove insoluble inorganic salts. The solution was evaporated to dryness under reduced pressure. The crude product was chromatographed to produce an orange solid in a 17% yield. ^1H NMR (400 MHz, DMSO-*d*6) δ 9.66 (d, *J*

= 8.0 Hz, 2H), 9.60 (d, *J* = 8.0 Hz, 2H), 8.68 (d, *J* = 2.9 Hz, 2H), 8.38 (dd, *J* = 5.2, 1.2 Hz, 2H), 8.32 (d, *J* = 8.4 Hz, 2H), 8.19 (dd, *J* = 8.0, 5.2 Hz, 2H), 8.01 (dd, *J* = 7.4, 1.0 Hz, 2H), 7.94 – 7.79 (m, 6H), 7.12 (td, *J* = 7.8, 0.8 Hz, 2H), 7.06 – 6.98 (m, 4H), 6.6 (dd, *J* = 7.4, 1.0 Hz, 2H). MALDI-TOF (M-PF_6^-): 884.985 (885.352).

[Ir(ppy)$_2$(tpphz)Ir(ppy)$_2$](PF$_6$)$_2$ (Ir2). The equiv of $[Ir(ppy)_2Cl]_2$ and tpphz was changed to 1:1.2 to obtain the dinuclear complex. Orange solid. Yield: 65%. ^{1}H NMR (400 MHz, $CDCl_3$) δ 10.32 (dd, *J* = 8.0, 0.8 Hz, 4H), 8.65 (dd, *J* = 5.2, 0.8 Hz, 4H), 8.36 (dd, *J* = 8.0, 5.2, Hz, 4H), 8.29 (d, *J* = 8.0 Hz, 4H), 7.96 (d, *J* = 8.0 Hz, 8H), 7.87 (d, *J* = 6.0 Hz, 4H), 7.12 (t, *J* = 7.8 Hz, 4H), 6.98-7.05 (m, 8H), 6.47 (d, *J* = 7.6 Hz, 4H). ^{13}C NMR (100 MHz, DMSO) δ 167.30, 152.87, 150.06, 149.88, 149.85, 149.83, 144.51, 140.55, 139.35, 136.39, 131.64, 130.83, 130.57, 129.16, 125.63, 124.35, 123.06, 120.53. MALDI-TOF (M-PF_6^-): 1530.698 (1530.542).

Photophysical properties

Table S1 Photophysical data for **Ir1** and **Ir2**

Complexes	λ_{abs} / nm (logarithmic absorption coefficients, log [ε])	λ_{em} / nm	Φ / %	Lifetime (N_2) / ns
Ir1	280 (4.5), 376 (4.0), 395 (4.1)	597	0.16	418
Ir2	275 (4.8), 380 (4.2)	609	0.06	646

Calculation results

Table S2 Calculated HOMO and LUMO of **Ir1** and **Ir2**

Complexes	**HOMO**	**LUMO**
Ir1	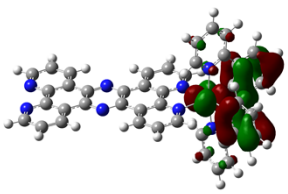	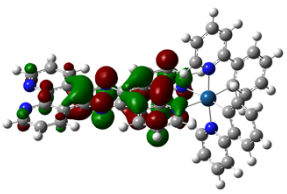
	-5.68ev	-2.13ev
Ir1-t	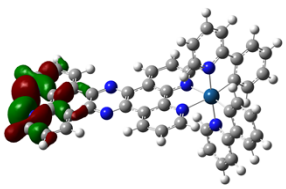	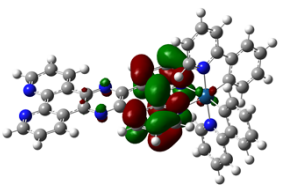
	-5.27ev	-1.78ev
Ir2	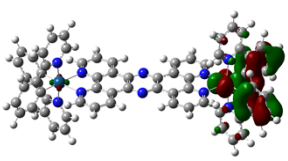	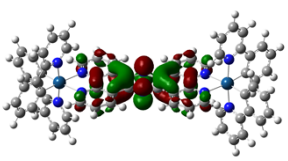
	-4.85ev	-1.20ev
Ir2-t	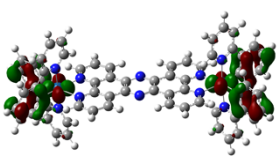	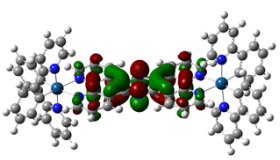
	-5.70ev	-2.05ev

Table S3 Absorption of **Ir1** and **Ir2** in CH_2Cl_2 solution from TD-DFT calculations.

Complexes	States	λ (nm)	E (eV)	Oscillator	Major Configurations (CI coeff)	Assignment
Ir1	S_1	418	2.97	0.0228	HOMO→LUMO (0.70)	MLCT/ILCT
Ir2	S_1	577	2.15	0.0002	HOMO→LUMO (0.68)	MLCT/ILCT
	S_7	442	2.81	0.0417	HOMO-2→LUMO (0.68)	

Table S4 Calculated phosphorescent emission of **Ir1** and **Ir2** in CH_2Cl_2 solution with the TD-DFT method.

Complexes	State	λ (nm)/E (eV)	Major Configurations	Character
Ir1	T_1	643/1.93	HOMO→LUMO (0.64)	^{3}MLCT/^{3}ILCT
Ir2	T_1	651/1.90	HOMO→LUMO (0.70)	^{3}MLCT/^{3}ILCT

Cell culture

MCF-7 cells and Hela cells were cultured in Dulbecco's modified Eagle's medium (DMEM) supplemented with 10% FBS. HepG 2 cells were cultured in RPMI-1640 supplemented with 10% FBS. All cells were cultured at 37 °C under 5% CO_2.

Cytotoxicity assay

The *in vitro* cytotoxicity toward MCF-7, Hela and HepG 2 cells was measured using the methyl thiazolyl tetrazolium (MTT, Beyotime) assay. First, cells were subcultured into 96-well cell-culture plate at a density of 1×10^4/well for 24 h before treatment. The treatment groups of complexes **Ir1** and **Ir2** (200 μL/well) were at concentrations of 5, 10, 25, 50, 75 and 100 μM, respectively, and the negative control groups were 200 μL/well DMSO diluted in culture reagents at final concentration of 0.1%, 0.5% and 1%, respectively. The two groups were added subsequently. The cells were incubated at 37 °C under 5% CO_2 for 24 h. The MTT (5 mg/mL) in PBS solution was added to each well of the two groups of 96-well assay plate, and incubated for another 4 h. An enzyme-linked immunosorbent assay (ELISA) reader (BioTek Instruments, Rower Wave XS2) was used to measure the OD570 (Absorbance value) of each well referenced at 570 nm. The viability of cell growth was calculated by the following formula: Viability (%) = (mean of Absorbance value of treatment group/mean Absorbance value of control) × 100.

Table S5 *In vitro* cytotoxicity of the complexes determined by the MTT assay.

Concentration		**Ir1**			**Ir2**	
(μM)	MCF-7	Hela	HepG 2	MCF-7	Hela	HepG 2
0	100	100	100	100	100	100
5	94.0 ± 1.7	95.1 ± 3.7	93.1 ± 2.1	97.8 ± 1.4	97.2 ± 1.6	96.6 ± 1.1
10	88.1 ± 3.6	89.1 ± 1.9	86.0 ± 1.0	93.5 ± 4.5	92.2 ± 4.2	90.5 ± 3.8
25	82.8 ± 1.8	83.2 ± 2.8	81.9 ± 3.5	89.1 ± 3.1	90.5 ± 2.7	87.6 ± 1.0
50	80.6 ± 1.8	81.3 ± 3.3	79.4 ± 2.1	85.5 ± 2.5	86.1 ± 0.7	84.7 ± 1.3
75	76.5 ± 0.8	72.7 ± 1.6	70.8 ± 3.3	80.8 ± 4.5	80.7 ± 2.5	81.5 ± 2.1

Luminescence imaging

Cells used for imaging were first incubated in culture dishes (3×10^8/L) until their adherence. The cells were washed with PBS three times and then incubated with 10 μM iridium(III) complexes in DMSO/culture reagents (1:99, v/v) for 1 h at 37 °C under 5% CO_2. Cell imaging experiments were then performed after the cells were washed with PBS for three times. In order to investigate the colocalization of **Ir1** and Hoechst 33342, HepG 2 cells were cultured with 10 μM **Ir1** in DMSO/culture reagents (1:99, v/v) for 1 h at 37 °C, and then further cultured with Hoechst 33342 (10 μg/mL) for another 10 min in

living cells. In fixed cells, the cells were fixed with 4% paraformaldehyde at room temperature for 20 min before staining with **Ir1** and Hoechst 33342. The mechanism investigation was performed with cells incubated under three different conditions: (1) the cells were incubated with **Ir1** under 4 ^{o}C for 1 h; (2) the cells were pretreated with 50 mM 2-deoxy-D-glucose and 5 μM oligomycin for 1 h at 37 ^{o}C; (3) the cells were pretreated with 50 mM NH_4Cl 1 h at 37 ^{o}C. In conditions of (2) and (3), the cells were then washed with PBS for three times and incubated with the solution of **Ir1** (10 μM) for another 1 h.

Luminescence imaging was performed with an Olympus IX81 laser scanning confocal microscope and a 40× objective lens. Cells incubated with the iridium(III) complexes were excited at 405 nm with a semiconductor laser, and the emission was measured according to the spectral data. The images were accomplished using the software package provided by Olympus instruments.

Photoluminescence lifetime imaging microscopy and time-gated luminescence imaging techniques were adopted on the platform afforded by Olympus IX81 laser scanning confocal microscope and PicoQuant Company. The objective lens was 40× and the frequency was 2.5 MHz for **Ir1**. The correlative calculations of the data were carried out with the software provided by PicoQuant.

The tracking of the distribution of Ir2 in cell cycle of Hela cells

The different locations of **Ir1** and **Ir2** in cells were interesting. As the limitans between the cytoplasm and the nucleus, the nuclear envelope might hinder **Ir2** entering the nucleus. Cell cycle synchronization of Hela cells with **Ir2** staining were performed to confirm the theroy. After pre-incubation with colchicine (0.5 μg/mL) for 8 h, Hela cells were delayed at mitosis metaphase (M phase: the nuclear envelope disintegrates in the late mitosis a short time). DMEM containing colchicine was replaced with fresh DMEM, cells were back to the normal cell cycle. Confocal images were taken at different time-points (M: 0.5 h, G1: 5.5 h, S: 16.5 h and G2: 21 h). **Fig. S1** showed that, during the M phase, when the nuclear envelope disintegrated, **Ir2** stained the whole cells uniformity. As the time went by, the area of phosphorescence of **Ir2** in nuclei was more and more samll (G1 and S phase). When cells in the G2 phase, **Ir2** mainly stained the cytoplasm, consistent with the previous results. This evidence indicated that nuclear envelope prevented **Ir2** entering the cell nuclei.

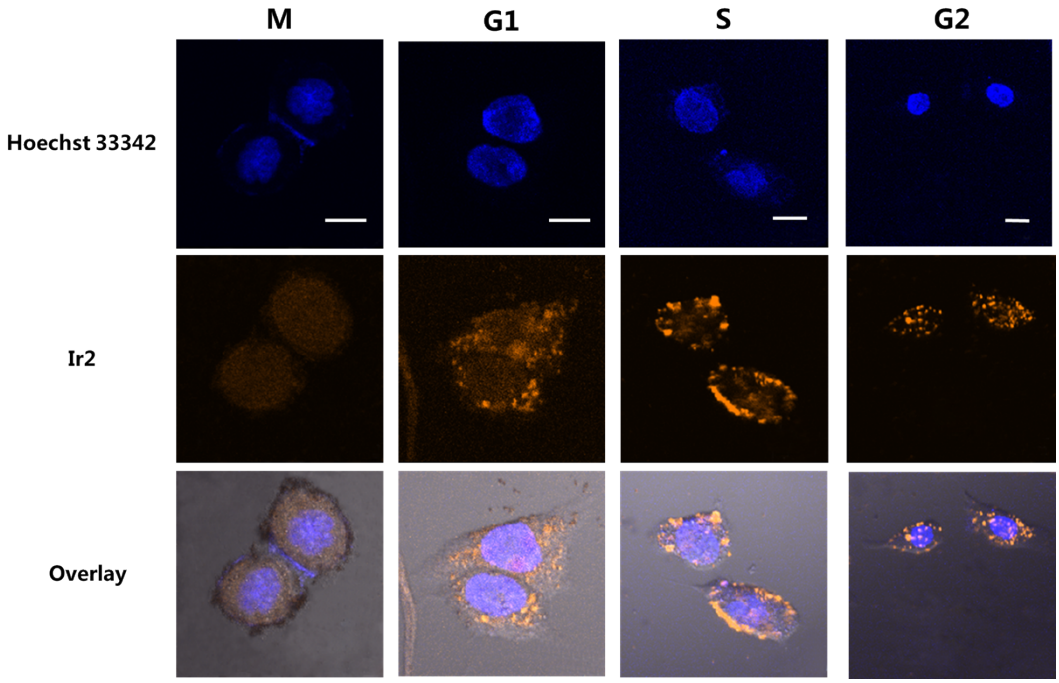

Fig. S1 Confocal images of living Hela cells incubated with 10 μM **Ir2** for 1h at 37 °C after release from colchicine at different time-points (M: 0.5 h, G1: 5.5 h, S: 16.5 h and G2: 21 h). Excitation wavelength was 405 nm. The emission of Hoechst 33342 and **Ir2** was collected at 420 – 490 nm and 550 – 650 nm, respectively. The scale bars were all 20 μm.

Mechanism of the cellular uptake of Ir1

To investigate the mechanism of cellular uptake of **Ir1**, a series of experiments were performed (**Fig. S2**). First, to ensure whether **Ir1** was taken up via a passive or active transport mechanism, HepG 2 cells were incubated with the solution of **Ir1** for 1 h at 4 °C. From **Fig. S2a**, we could observe weak luminescence in the cells when the cells were incubated at 4 °C. **Fig. S2b** showed the average intensity of nuclei of the cells. HepG 2 cells preincubated with metabolic inhibitors (50 mM 2-deoxy-D-glucose and 5 μM oligomycin), which could inhibit the active transport,[1] displayed weak luminescence, which indicated that the cellular uptake of **Ir1** was energy-dependent. As endocytosis is the most common energy-dependent cell uptake pathway,[2] the effect of NH_4Cl, a well-documented inhibitor of endocytosis, on the cellular uptake of **Ir1** was studied. Pretreatment of the cells with NH_4Cl did not alter the staining pattern of **Ir1**. In addition, the endocytotic pathway is usually a slow process.[3] However, the kinetic tracking experiment showed that the cellular uptake of **Ir1** reached the balance within 12 min (**Fig. S3**). The above results revealed that **Ir1** entered cells through an energy-dependent and non-endocytotic pathway.

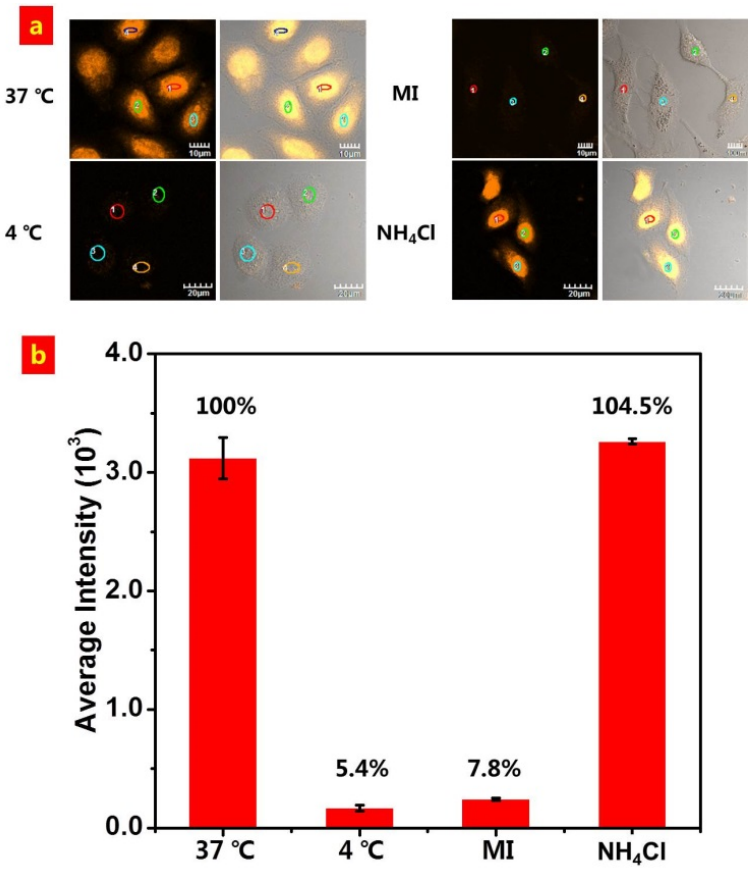

Fig. S2 (a) Confocal imaging of HepG 2 cells under different conditions. 37 ^{o}C (normal condition): the cells were incubated with **Ir1** at 37 ^{o}C for 1 h; 4 ^{o}C: the cells were incubated with **Ir1** at 4 ^{o}C for 1 h; MI (Metabolic inhibitors): the cells were preincubated with 50 mM 2-deoxy-D-glucose and 5 μM oligomycin for 1 h and then incubated with **Ir1** at 37 ^{o}C for 1 h; NH_4Cl: the cells were preincubated with 50 mM NH_4Cl for 1 h and then incubated with **Ir1** at 37 ^{o}C for 1 h. The scale bars of these different conditions were 10 μm, 20 μm, 10 μm and 20 μm, respectively. (b) The average intensity of those assigned areas in the different conditions.

Kinetic tracking of cellular uptake of Ir1

The dynamic process of **Ir1** staining the nucleus was monitored in real time by continuous imaging of live HepG 2 cells (**Fig. S3**). Live cells workstation was used to afford the appropriate temperature and atmosphere. We took a photo before starting the continuous imaging to assure that the autofluorescence of cells could not be detected. Then we replaced the medium with the solution of **Ir1** (10 μM). Weak luminescence was observed when taking a photo at T_0 (T_0 < 30 s, a relatively short time for cells entering the focal plane of the objective lens) in the cytoplasm. About 100 s and longer, distinct luminescence was catched in the nuclei. As the time went by, the averge intensity of nucleus was higher than the cytoplasm. After 700 s, the curves of the averge intensities of cytoplasm and nucleus were lever off to parallel. So we

could get the conclusion that **Ir1** entered the nucleus within 12 min.

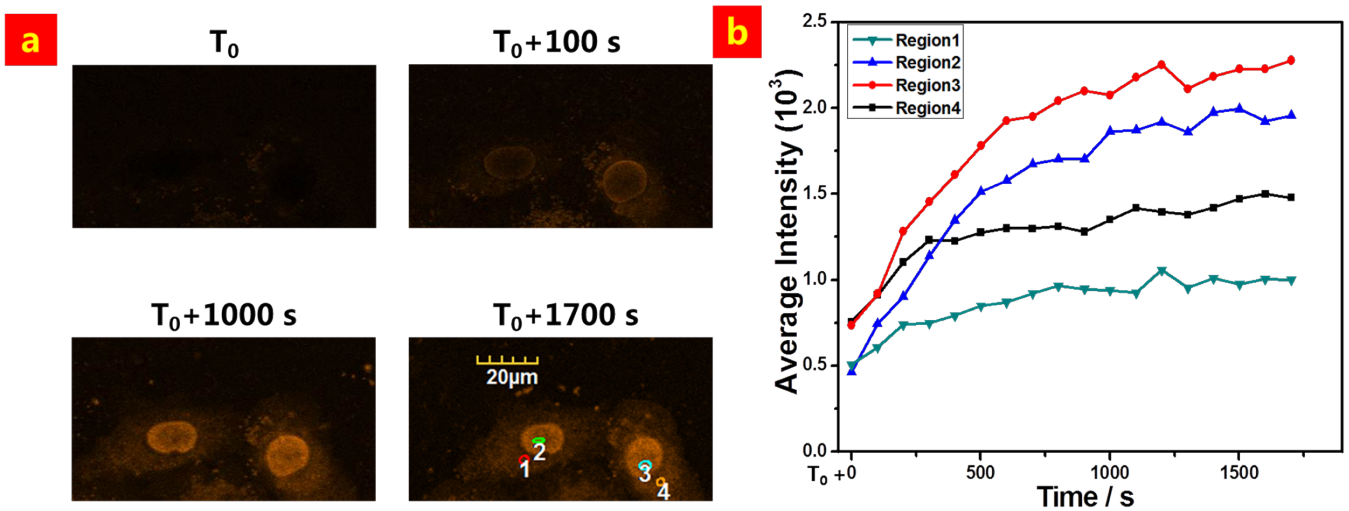

Fig. S3 Real-monitoring of nuclear staining with **Ir1**. (a) Luminescence images captured at the selected time. (b) Time course of average luminuscence intensity of the selected areas (Region 1 and Region 4 were in cytoplasm, and Region 2 and Region 3 were in nucleus.). Photoexcitation wavelength was 405 nm.

Photostability

a

Excitation Time (s)	Intensity Percentage (%)	
	Hoechst 33342	Ir1
0	100	100
0.1	60.5	98.6
0.3	25.5	91.5
0.5	7.4	89.9
0.8	4.8	88.3
1	0	81.9
1.5	0	80.0
3	0	57.6
6	0	51.7
15	0	32.2
30	0	13.7
50	0	10.0

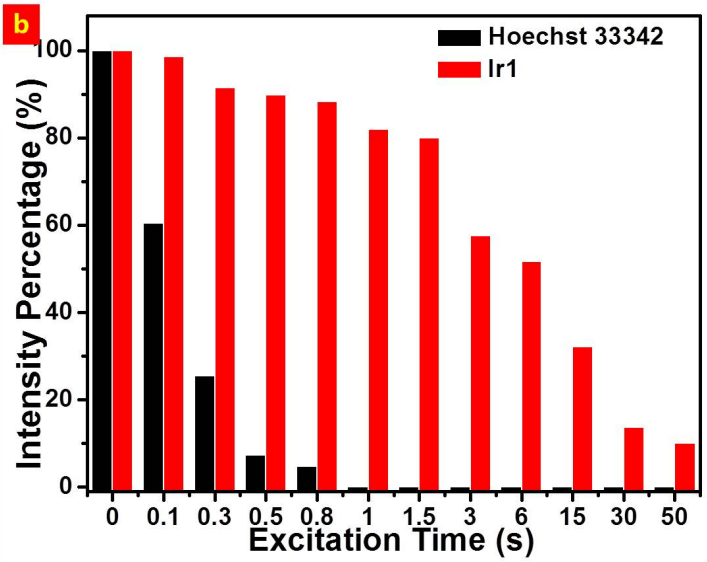

Fig. S4 The intensity percentage of Hoechst 33342 and **Ir1** after different irradiation time. The HepG 2 cells were incubated with **Ir1** for 1 h at 37 ºC and then further incubated with Hoechst 33342 for 10 min. The concentrations of **Ir1** and Hoechst 33342 in incubation solution were 10 μM and 10 μg/mL, respectively. Excitation wavelength was 405 nm. The bleach experiment was performed under tornado mode.

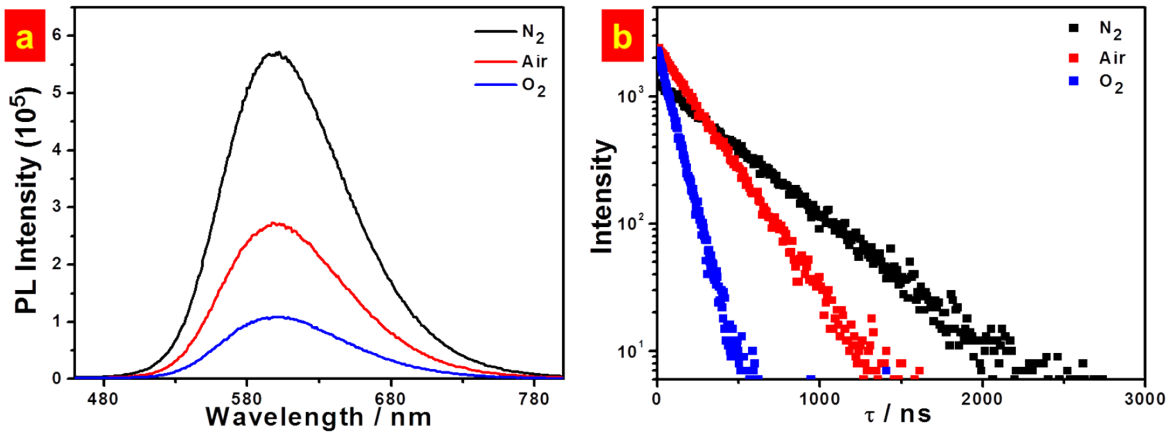

Fig. S5 The response of emission intensity (a) and emission lifetime (b) of **Ir1** to the oxygen contents in dichloromethane at 298 K ($\tau(O_2)$ = 84 ns, τ(Air) = 223 ns, $\tau(N_2)$ = 418 ns).

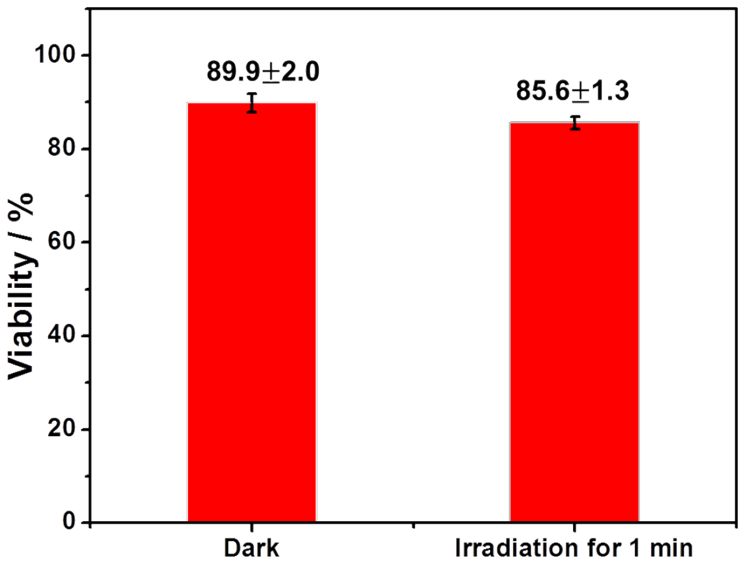

Fig. S6 Cell viability of Hela cells incubated with **Ir1** (10 μM) by using typical MTT assay under dark or under 405 nm light irradiation for 1 min. The irradiation power of 405 nm (generated by semiconductor laser) is 5 mW/cm^2.

References

1 (*a*) C. A. Puckett and J. K. Barton, *Biochemistry*, 2008, **47**, 11711; (*b*) K. Y. Zhang and K. K. Lo, *Inorg. Chem.*, 2009, **48**, 6011; (*c*) K. Y. Zhang, H. W. Liu, T. T. Fong, X. G. Chen and K. K. Lo, *Inorg. Chem.*, 2010, **49**, 5432.

2 S. E. Gratton, P. A. Ropp, P. D. Pohlhaus, J. C. Luft, V. J. Madden, M. E. Napier and J. M. DeSimone, *Proc. Natl. Acad. Sci. U. S. A.*, 2008, **105**, 11613.

3 (*a*) M. S. Cartiera, K. M. Johnson, V. Rajendran, M. J. Caplan and W. M. Saltzman, *Biomaterials*, 2009, **30**, 2790; (*b*) H. Jin, D. A. Heller and M. S. Strano, *Nano Lett.*, 2008, **8**, 1577.